

A EUROPEAN JOURNAL

CHEMPHYSICHEM

OF CHEMICAL PHYSICS AND PHYSICAL CHEMISTRY



Reprint

© Wiley-VCH Verlag GmbH & Co. KGaA, Weinheim

A Journal of



WILEY-VCH

www.chemphyschem.org

Reactivity of the Indenyl Radical (C_9H_7) with Acetylene (C_2H_2) and Vinylacetylene (C_4H_4)

Long Zhao,^[a] Matthew B. Prendergast,^[a] Ralf I. Kaiser,^{*[a]} Bo Xu,^[b] Wenchao Lu,^[b] Utuq Ablikim,^[b] Musahid Ahmed,^{*[b]} Artem D. Oleinikov,^[c] Valeriy N. Azyazov,^[c] Alexander M. Mebel,^{*[c, d]} A. Hasan Howlader,^[d] and Stanislaw F. Wnuk^[d]

The reactions of the indenyl radicals with acetylene (C_2H_2) and vinylacetylene (C_4H_4) is studied in a hot chemical reactor coupled to synchrotron based vacuum ultraviolet ionization mass spectrometry. These experimental results are combined with theory to reveal that the resonantly stabilized and thermodynamically most stable 1-indenyl radical ($C_9H_7^*$) is always formed in the pyrolysis of 1-, 2-, 6-, and 7-bromoindenes at 1500 K. The 1-indenyl radical reacts with acetylene yielding 1-ethynylindene plus atomic hydrogen, rather than adding a second acetylene molecule and leading to ring closure and formation of fluorene as observed in other reaction mechanisms such as the hydrogen abstraction acetylene addition or hydro-

gen abstraction vinylacetylene addition pathways. While this reaction mechanism is analogous to the bimolecular reaction between the phenyl radical ($C_6H_5^*$) and acetylene forming phenylacetylene (C_6H_5CCH), the 1-indenyl + acetylene \rightarrow 1-ethynylindene + hydrogen reaction is highly endoergic (114 kJ mol^{-1}) and slow, contrary to the exoergic (-38 kJ mol^{-1}) and faster phenyl + acetylene \rightarrow phenylacetylene + hydrogen reaction. In a similar manner, no ring closure leading to fluorene formation was observed in the reaction of 1-indenyl radical with vinylacetylene. These experimental results are explained through rate constant calculations based on theoretically derived potential energy surfaces.

1. Introduction

Resonantly stabilized free radicals (RSFR) have been implicated in high temperature and pressure environments prevalent in combustion and astrochemical systems. These RSFR's can lead to molecular growth, and polycyclic aromatic hydrocarbon formation upon reaction with hydrocarbons prevalent in such environments.^[1] While much attention has been paid to smaller RSFR's such as the propargyl and allyl radicals, there is paucity in formation of and further growth from larger radicals such as indenyl. This is surprising since the indene molecule (C_9H_8) itself has received considerable attention from the combustion and physical (organic) chemistry communities^[2] as a potential building block of non-planar polycyclic aromatic hydrocarbons (PAHs) such as corannulene ($C_{20}H_{10}$) – a precursor to fullerenes

such as C_{60} and C_{70} (Scheme S1 in the Supporting Information).^[3] Moreover, the RSFR's containing five-membered rings like indenyl have been speculated as the driving force for PAH nucleation leading eventually to the formation of soot particles.^[1]

Indene – the prototype of an aromatic compound carrying one six- and one five membered ring – has been identified in sooting flames of non-aromatic hydrocarbon-based fuels like methane (CH_4),^[4] ethane (C_2H_6),^[5] acetylene (C_2H_2),^[6] propene (C_3H_6),^[7] *n*-butane (C_4H_{10}),^[8] 1,3-butadiene (C_4H_6),^[9] as well as in aromatic fuels such as benzene (C_6H_6),^[10] toluene (C_7H_8),^[6,11] styrene (C_8H_8),^[10] ethylbenzene (C_8H_{10}),^[10] and xylenes (C_8H_{10}).^[10,12] Recently, indene formation was proposed to also involve methyl radical (CH_3^*) reactions with toluene (C_7H_8) followed by cyclization and dehydrogenation of the initial collision complex.^[21] The results from pyrolysis of cyclopentadienyl (C_5H_5) as conducted by Mulholland and coworkers^[12a] were explained by Wang et al.^[13] theoretically. They showed that intra molecular addition pathways dominate at low temperatures resulting in indene formation with higher branching ratios than those of naphthalene ($C_{10}H_8$) and benzene (C_6H_6). Marinov et al. conducted flame tests with *n*-butane and detected indene as well.^[8] Formation of (methylated) indene through the reactions of the C_3H_4 isomers allene (H_2CCCH_2) and methylacetylene (CH_3CCH) with (methyl substituted) phenyl radicals ($C_6H_5^*$) (Scheme S2 in Supplementary Information) has been reported,^[29, h, 14] while indene was also formed via a directed synthesis through benzyl radical ($C_6H_5CH_2^*$) reactions with acetylene (C_2H_2).^[2f, g]

However, the further PAH growth beginning from indene has remained largely unexplored as experimental studies of the reactivity of indenyl radicals (1H-inden-1-yl, $C_9H_7^*$) have been

[a] Dr. L. Zhao, Dr. M. B. Prendergast, Prof. Dr. R. I. Kaiser
Department of Chemistry
University of Hawaii at Manoa
Honolulu, Hawaii, 96822 (USA)
E-mail: ralfk@hawaii.edu

[b] Dr. B. Xu, Dr. W. Lu, Dr. U. Ablikim, Dr. M. Ahmed
Chemical Sciences Division
Lawrence Berkeley National Laboratory
Berkeley, CA 94720 (USA)
E-mail: mahmed@lbl.gov

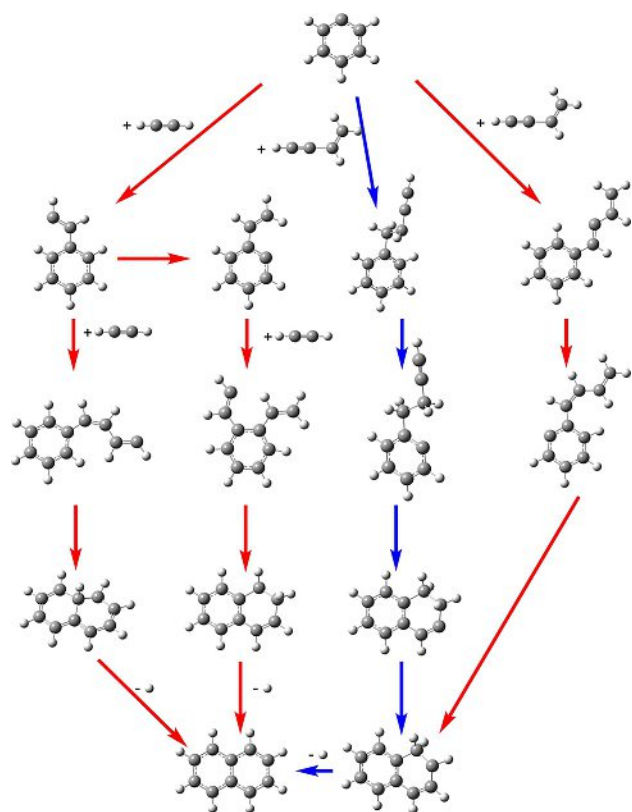
[c] A. D. Oleinikov, Prof. Dr. V. N. Azyazov, Prof. Dr. A. M. Mebel
Samara National Research University
Samara 443086 (Russia)
E-mail: mebela@fiu.edu

[d] Prof. Dr. A. M. Mebel, A. H. Howlader, Prof. Dr. S. F. Wnuk
Department of Chemistry and Biochemistry
Florida International University
Miami, FL 33199 (USA)

Supporting information for this article is available on the WWW under <https://doi.org/10.1002/cphc.201900052>

limited to its reaction with singlet carbene (CH_2),^[15] the barrierless recombination with a hydrogen atom (H) to indene,^[15] the reaction with the hydroperoxy radical (HO_2) forming indenoxyl radical ($\text{C}_9\text{H}_7\text{O}^\bullet$) plus hydroxyl radical (OH^\bullet),^[16] and the reaction with acetylene (C_2H_2) leading to a $\text{C}_9\text{H}_7\text{CHCH}$ complex via a barrier to addition of about 54 kJ mol^{-1} .^[17] Spectroscopic investigations of indenyl radicals are even sparser. Using electron impact ionization, Pottie and Lossing^[18] deduced an adiabatic ionization energy (AIE) of the 1H-indenyl as 8.35 eV while a vacuum ultraviolet (VUV) photoionization study by Fischer et al.^[19] determined the AIE to be 7.53 eV and identified an excited $^3\text{B}_2$ state of the cation at 8.10 eV. Another VUV study reports the AIE of 7.48 eV^[20] and an estimate for the enthalpy of formation of the neutral radical $\Delta_f H^\circ_{0\text{K}}$ of $249 \pm 50 \text{ kJ mol}^{-1}$.^[21]

Hydrogen abstraction-acetylene addition (HACA) and hydrogen abstraction-vinylacetylene addition (HAVA) mechanisms have been implicated in combustion environments to drive aromatic ring formation and a stepwise growth of larger PAH. For instance, starting with the phenyl radical ($\text{C}_6\text{H}_5^\bullet$), the HACA sequence leads in successive reactions with acetylene (C_2H_2) to naphthalene (C_{10}H_8) at elevated temperatures (Scheme 1).^[22] In a similar manner, phenyl radical derivative reactions with vinylacetylene (C_4H_4) revealed a de-facto barrier-less reaction to



Scheme 1. Naphthalene formation via the hydrogen abstraction-acetylene addition (HACA) route and the hydrogen abstraction-vinylacetylene addition (HAVA) pathway. Pathways color coded in blue and red have no entrance barrier or a barrier to addition, respectively.

(methyl substituted) naphthalene (C_{10}H_8) along with atomic hydrogen (H) via the HAVA pathway (Scheme 1).^[23]

Here, we explore to what extent the concepts of the HACA and HAVA pathways can be exported to molecular mass growth processes from indenyl radicals under combustion-like conditions. This requires an intimate understanding of the formation and isomerization of indenyl radicals and also of the reactivity of indenyl radicals with simple, but ubiquitous hydrocarbon reactants such as acetylene (C_2H_2) and vinylacetylene (C_4H_4). In this work, we report first on the initial generation of 1-indenyl radicals ($\text{C}_9\text{H}_7^\bullet$) exploiting synchrotron-based photoionization – reflectron time of flight mass spectrometry.^[24] Thereafter, we explore the reactivity of the 1-indenyl radical with acetylene (C_2H_2) and vinylacetylene (C_4H_4) as a possible first step leading to a growth of PAHs carrying a five-membered ring starting with indenyl(y) species.

2. Results and Discussion

2.1. Computational Results

Our computations reveal that the C_{2v} symmetric and RFSR species 1-indenyl ($\text{C}_9\text{H}_7^\bullet$; $^2\text{A}_2$) represents the thermodynamically most stable isomer of the indenyl family (Figure 1). The 2- and 3-indenyl radicals, which can be formally derived from hydrogen abstraction processes from the CH moiety at the C2 and C3 atom of the indene molecule at the cyclopentadiene ring are less stable by 144 and 145 kJ mol^{-1} due to the lack of resonance

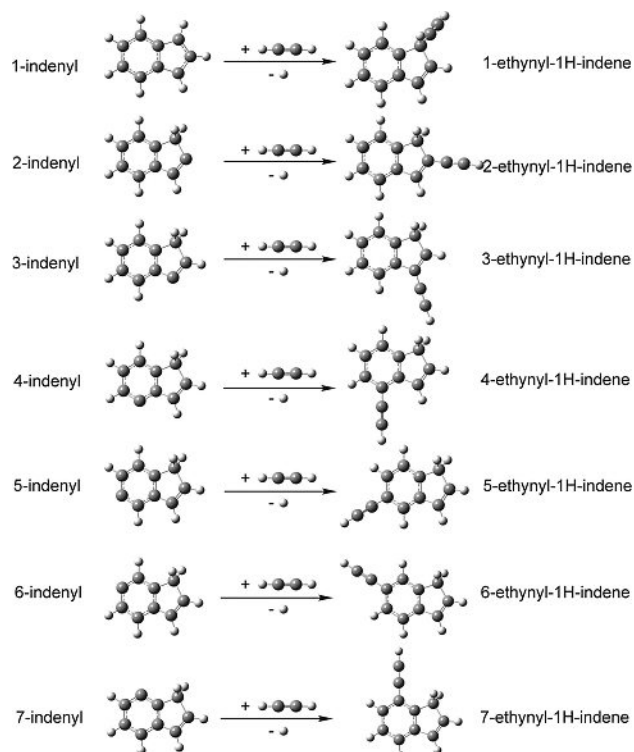


Figure 1. Acetylene addition to distinct indenyl radicals leading to the corresponding ethynylindene isomers.

stabilization of the resulting radical. Likewise, the aryl-type 4-, 5-, 6-, and 7-indenyl radicals are less stable by 133, 132, 133, and 132 kJ mol^{-1} compared to the 1-indenyl radical. This results in carbon-hydrogen (C–H) bond strengths of 327, 471, 471, 460, 459, 460, and 459 kJ mol^{-1} to form the corresponding 1- to 7-indenyl radicals from the indene molecule. The corresponding AIEs for the 1- to 7-indenyl radicals were determined to be 7.40 eV, 7.97 eV, 7.95 eV, 7.67 eV, 7.83 eV, 7.89 eV, and 7.66 eV. At the level of theory applied, the computed ionization energies are typically 0.05 eV to 0.15 eV lower compared to experimentally determined benchmarks.^[25] Considering these corrections, the computed AIE of 1-indenyl of 7.40 eV agrees – after correction to 7.45 eV to 7.55 eV – exceptionally well with the experimentally determined values of 7.53 eV (Fischer et al.^[19]) and 7.48 eV (Qi et al.^[20]).

With respect to the reaction of the indenyl radicals with acetylene via an acetylene addition–atomic hydrogen elimination pathway to synthesize distinct ethynylindene isomers (Figure 1), we computed overall reaction energies of +114, –58, –57, –43, –39, –40, and –42 kJ mol^{-1} synthesizing the 1-ethynylindene to 7-ethynylindene isomers, respectively, with barriers to addition of the radical center of the indenyl radical to the carbon-carbon triple bond of the acetylene molecule to be 60, 12, 11, 12, 14, 13, and 13 kJ mol^{-1} , respectively. Note that the strongly endoergic reaction of the 1-indenyl radical with acetylene yielding 1-ethynylindene plus atomic hydrogen can be associated with the loss of the resonance stabilization energy of the 1-indenyl radical upon formation of 1-ethynylindene. AIE's of 1-ethynylindene to 7-ethynylindene isomers were computed to be 8.13 eV, 7.85 eV, 8.06 eV, 8.02 eV, 8.06 eV, 7.88 eV, and 8.11 eV, which are once again expected to be 0.05 eV to 0.15 eV lower than the actual AIE's. Wentrup et al. determined the vertical ionization energy (VIE) of the 2-ethynylindene isomer to be 8.04 eV, which is close to the computed VIE of 7.99 eV.^[26]

The potential energy diagram for the reaction of 1-indenyl with acetylene is illustrated in Figure 2. The reaction with acetylene, after the formation of the initial addition complex **i1'**,

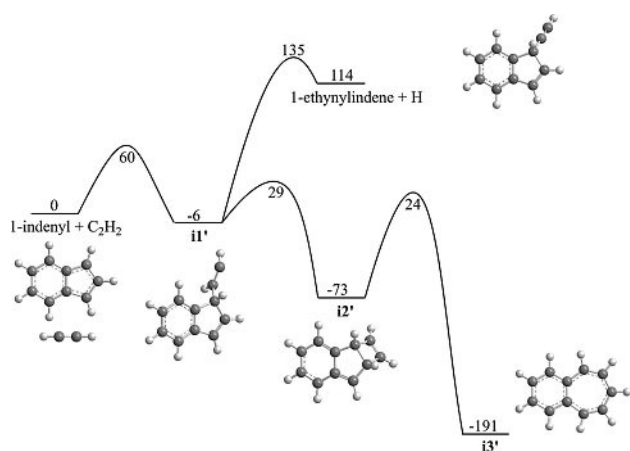


Figure 2. Calculated potential energy diagram for the 1-indenyl plus acetylene reaction. All relative energies are shown in kJ mol^{-1} .

proceeds either by a hydrogen atom loss to the endoergic product 1-ethynylindene via a barrier of 135 kJ mol^{-1} relative to the reactants or by the formation of a four-member ring in **i2'** followed by the expansion of fused five- and four-member rings producing intermediate **i3'** residing in a deep potential well (–191 kJ mol^{-1}) and containing joined six- and seven-member rings. It can be anticipated that the ultimate reaction outcome, i.e. the formation of the 1-ethynylindene + hydrogen bimolecular product versus collisional stabilization (thermalization) of **i3'** should strongly depend on the reaction temperature and pressure.

Figure 3 illustrates the potential energy diagram of representative channels for the 1-indenyl + vinylacetylene (C_4H_4) reaction. Vinylacetylene can add to 1-indenyl by either vinylic (C1 carbon) or acetylenic (C4 carbon) ends forming intermediates **i1** and **i2** via barriers of 39 and 41 kJ mol^{-1} , respectively. Next, hydrogen eliminations from the initial complexes can produce products 1-((E)-but-1-en-3-ynyl)-1H-indene (**p1**) and 1-(but-3-en-1-ynyl)-1H-indene (**p2**) endoergic by 115 and 111 kJ mol^{-1} , respectively, via 12–13 kJ mol^{-1} exit barriers. Since the addition of vinylacetylene by the $\text{H}_2\text{C}=\text{C}$ end has been shown to be more favorable for the formation of an additional six-member ring, for instance in the phenyl + vinylacetylene reaction,⁷ here we researched pathways for the ring closure leading to the exoergic products fluorene (**p3**) and 1H-cyclopenta[a]naphthalene (**p5**) beginning from the intermediate **i1**. The extra ring formation process begins with 1,3-H migration from the attacked carbon in the five-member ring to the β -C atom in the side chain producing **i3** via a transition state lying 98 kJ mol^{-1} above the initial reactants. Two reaction channels are found beginning with **i3**. The first one starts with a 1,2-H shift in the five-member ring to **i4**, continues via a facile six-member ring closure giving **i5** and another 1,2-H shift from the CH_2 group to the bare carbon atom in the newly formed ring producing **i6**, and completes by an atom loss from the CH_2 moiety in the new six-member ring forming fluorene **p3** as the final product. The first step on this pathway, the hydrogen migration within the five-member is critical as it proceeds via the highest barrier, with the corresponding transition state residing as high as 213 kJ mol^{-1} above 1-indenyl + vinylacetylene. The alternative channel from **i3** involves more steps but is more favorable energetically. It begins with five-member ring closure leading to a spirane-like intermediate **i7** via a relatively low barrier (9 kJ mol^{-1} above the reactants). Next, **i7** features a 1,2-H shift in the new five-member ring forming another, much more stable spirane intermediate **i8** and the latter rearranges to a tetracyclic intermediate **i9** containing one six-, two five-, and one three-member fused rings. Ring expansion in **i9** can go in two different ways, to **i10** where the five-member ring in the middle and the three-member ring form a new six-member ring or to **i11** in which a new six-member ring forms in the vicinal position from the vicinal five-member and three-member rings. The intermediate **i10** dissociates to the 1H-cyclopenta[a]naphthalene **p5** product by hydrogen loss, whereas **i11** is subjected to an additional 1,2-H shift step to **i6**, which in turn decomposes to fluorene. In addition to the formation of highly exoergic fluorene (–173 kJ mol^{-1}) and 1H-cyclopenta[a]

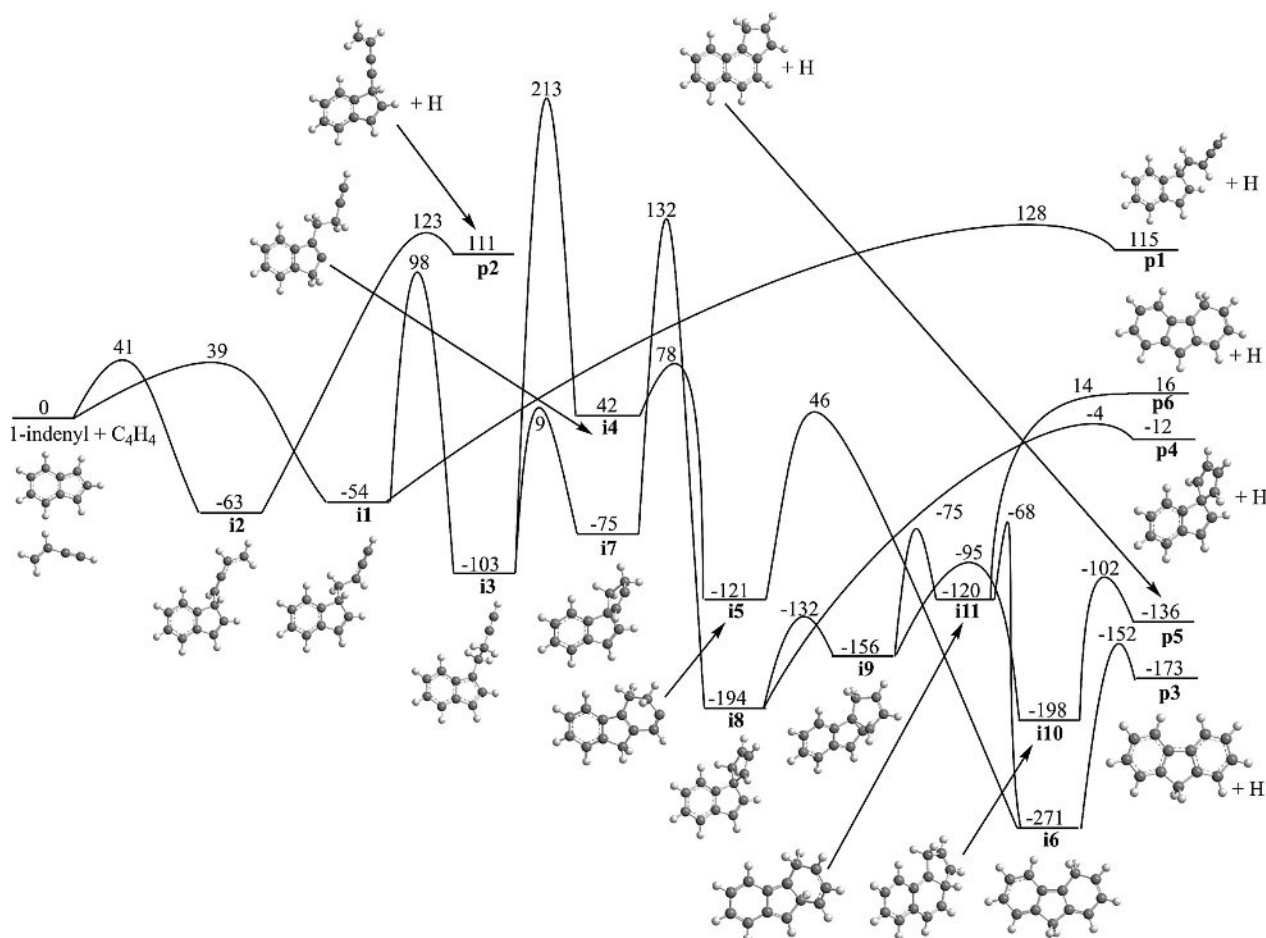


Figure 3. Calculated potential energy diagram for the 1-indenyl plus vinylacetylene reaction. All relative energies are shown in kJ mol^{-1} .

naphthalene (-136 kJ mol^{-1}), the reaction channel via **i7** can also give a slightly exoergic product **p4** (benzospirane, -12 kJ mol^{-1}) and endoergic **p6** ($+16 \text{ kJ mol}^{-1}$) by hydrogen atom eliminations from **i8** and **i11**, respectively. The rate-limiting step on the pathway involving **i7** is **i7**→**i8** with the transition state lying 132 kJ mol^{-1} higher in energy than 1-indenyl + vinylacetylene. As compared to the straightforward hydrogen loss path to form **p1**, the channel producing fluorene (-173 kJ mol^{-1}) and 1*H*-cyclopenta[*a*]naphthalene features a slightly higher critical barrier (132 vs. 128 kJ mol^{-1}) and also is much less favorable in terms of the high entropy demands. Therefore, it can be anticipated that the 1-indenyl plus vinylacetylene reaction is controlled kinetically and would produce predominantly **p1** at high temperatures rather than highly exoergic tricyclic PAH products **p3** and **p5**. In the meantime, the critical reaction barriers are so high, 123 – 132 kJ mol^{-1} , that the reaction would be expected to be slow.

2.2. Experimental Results

Characteristic mass spectra recorded at a photoionization energy of 10.00 eV for the acetylene seeded 1-bromoindene, 2-

bromoindene, 6-bromoindene, and 7-bromoindene systems at a temperature of the silicon carbide tube of $1500 \pm 10 \text{ K}$ are displayed in Figures 4a–d. These spectra reveal ion counts of singly ionized bromoindene precursors ($\text{C}_9\text{H}_7^{79}\text{Br}/\text{C}_9\text{H}_7^{81}\text{Br}$; $m/z = 194/196$). Signals at mass-to-charge ratios (m/z) of 117 ($^{13}\text{CC}_8\text{H}_8^+$), 116 ($\text{C}_9\text{H}_8^+ / ^{13}\text{CC}_8\text{H}_7^+$), and 115 (C_9H_7^+) are observable in each system as well. These ion counts can be linked to non-pyrolyzed bromoindene precursors ($m/z = 194/196$) and to the indene molecule ($m/z = 116$) along with its ^{13}C counterpart ($m/z = 117$); indene molecules can be formed in the reactor via barrier-less recombination of atomic hydrogen and any indenyl radical followed by third body stabilization of the adduct to indene. Signal at $m/z = 115$ can be associated with ionized indenyl radicals (C_9H_7^+). Additional ion counts at $m/z = 140$ ($\text{C}_{11}\text{H}_8^+$) can be linked to reactions within the indenyl (C_9H_7^+ ; 115 amu)-acetylene (C_2H_2 ; 26 amu) systems leading to a molecule of the formula C_{11}H_8 (140 amu) along with atomic hydrogen (H ; 1 amu) [Reaction (R1)]. The ^{13}C - and $^{13}\text{C}_2$ -substituted counterparts of C_{11}H_8 contribute to the signal at $m/z = 141$ ($^{13}\text{CC}_{10}\text{H}_8$) and 142 ($^{13}\text{C}_2\text{C}_9\text{H}_8$), respectively. Also, ion counts were detected at $m/z = 139$ ($\text{C}_{11}\text{H}_7^+$) (Figure S1 in Supplementary Information). It is important to note that under our experimental conditions, the addition of vinylacetylene

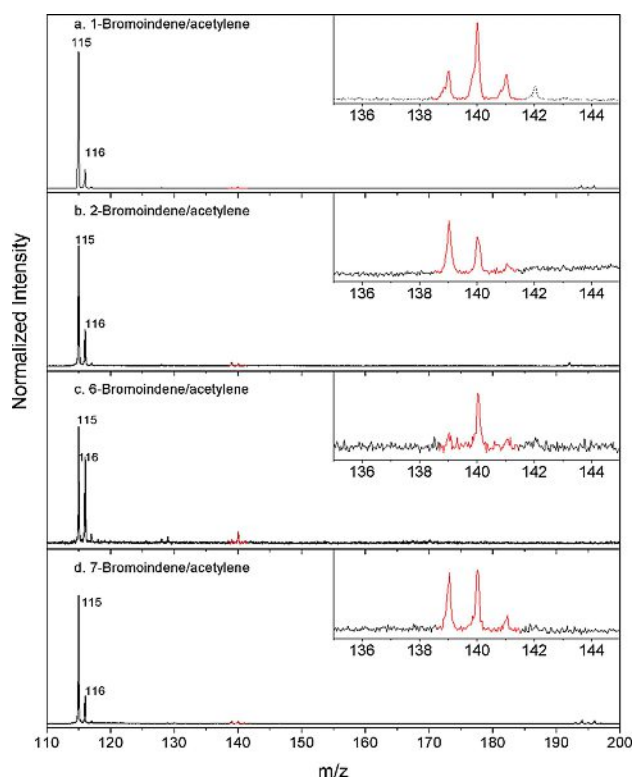


Figure 4. Mass spectra recorded at 10.00 eV and 1500 K from the reactions 1-bromoindene/acetylene (a), 2-bromoindene/acetylene (b), 6-bromoindene/acetylene (c), and 7-bromoindene/acetylene (d). Product signals in the inset show masses around $m/z = 140$ are highlighted in red.

(C_4H_4) to the pyrolyzed bromoindene precursors does not reveal any new ion peaks except $m/z = 52$ ($C_4H_4^+$) and 53 ($^{13}CC_3H_4^+$).



$C_9H_7^+$ (115 amu) and $C_{11}H_8$ (140 amu), are identified via analysis of their corresponding photoionization efficiency (PIE) curves, measured between 7.40 eV to 10.00 eV (Figures 5a–p). All four PIE curves of $m/z = 115$ ($C_9H_7^+$), are superimposable (Figures 3a, 3e, 3i and 3m) and depict an onset of the ion signal at 7.50 ± 0.05 eV. This onset compares well with the AIE of the 1-indenyl radical of 7.48–7.53 eV, and the literature PIE curves as determined by Fischer et al.^[19] and Qi et al.^[20] This suggests that the 1-indenyl radical is the dominant radical formed in the pyrolysis of all bromoindene precursors. Therefore, significant isomerization processes must exist in the 2-, 6-, and 7-indenyl radicals if those are formed via pyrolysis of their corresponding bromo-precursors; in an alternative scenario discussed in the subsequent Section, the 2-, 6-, and 7-indenyl radicals are not produced at all. The 1-indenyl radical can also be detected via its ^{13}C -labeled counterpart through $m/z = 116$ ($^{13}CC_8H_7^+$); here, signal at $m/z = 116$ can be fit for all four systems with two channels from ^{13}C -1-indenyl ($^{13}CC_8H_7^+$) along with indene (C_9H_8). It is important to note that the computed PIEs for the 1-indenyl radical – shifted by 0.1 eV as discussed above – correlate well with the experimental curve of $m/z = 115$ from 7.40 eV to

7.90 eV, but not beyond that. Here, a comparison of the plateau of the calculated curve beyond 7.90 eV with the experimentally determined PIE curves of the 1-indenyl radical is the result of excited electronic states, not considered here, such as the 3B_2 state in the indenyl cation at 8.10 eV in the computations, which would add additional intensity to the PIE curve (Figure S2a in the Supporting Information).

Now we consider the PIE curves for $m/z = 140$, which are essentially identical and reveal an onset of the ion counts at about 8.00 ± 0.10 eV. This onset (within the error bars of the computed values) could be associated with the formation of any of the seven ethynylindene isomers; note that the AIEs of distinct isomers of ethynylindenes are quite similar within our experimental error limits; this trend mirrors closely the findings for ethynyl-naphthalenes^[27] and ethynyl-phenanthrene isomers^[28] with AIEs falling within a narrow range of only 0.2 eV.^[29] The 1-indenyl radical represents the key reactant formed from 1-bromoindene upon pyrolysis, hence we predict that upon reaction with acetylene via Reaction (R1), the 1-ethynylindene product is formed. This mechanism could be operable for the remaining three systems, in which the 1-indenyl radical also represents the (dominating) reactant hence potentially leading to 1-ethynylindene. Therefore, we may conclude that the 1-indenyl radical and the 1-ethynylindene are formed in the bromoindene–acetylene systems, respectively. This is also supported from the comparison of the computed PIE curve of the 1-ethynylindene isomer with the experimental data of $m/z = 140$. None of the PIE curves of the remaining 2- to 7-ethynylindene isomers are able to replicate the experimental data (Figure S2b in the Supporting Information).

3. Discussion

The identification of the 1-indenyl radical suggests that if the 2-, 6-, and 7-indenyl radicals are formed via homolytic carbon–bromine bond rupture, these radicals effectively isomerize within a few tens of microseconds, i.e. the residence time of the radicals within our chemical reactor.^[14a,22–23,24,27,30] An alternative explanation for the non-observation of the 2-, 6-, and 7-indenyl radicals would be that they do not actually form in the first place from the bromoindenes used in the present experiment. Let us consider and compare both possible scenarios. If the n -indenyl radicals ($n > 1$) are initially produced from the precursors, two isomerization mechanisms can account for their disappearance: i) successive hydrogen shifts and ii) hydrogen atom assisted isomerization via a recombination of hydrogen atoms with the initially formed indenyl radicals leading to chemically activated indene molecules followed by unimolecular decomposition of indene to 1-indenyl plus atomic hydrogen. To evaluate the role of a hydrogen atom assisted isomerization, rate constant calculations for the reaction of the 1-, 2-, 6-, and 7-indenyl radical with atomic hydrogen and indene decomposition are provided (Figure 6). These computations reveal that the reactions of 1-, 2-, 6-, and 7-indenyl radicals with hydrogen rapidly produce either indene at low temperatures or predominantly 1-indenyl plus atomic hydrogen at high temper-

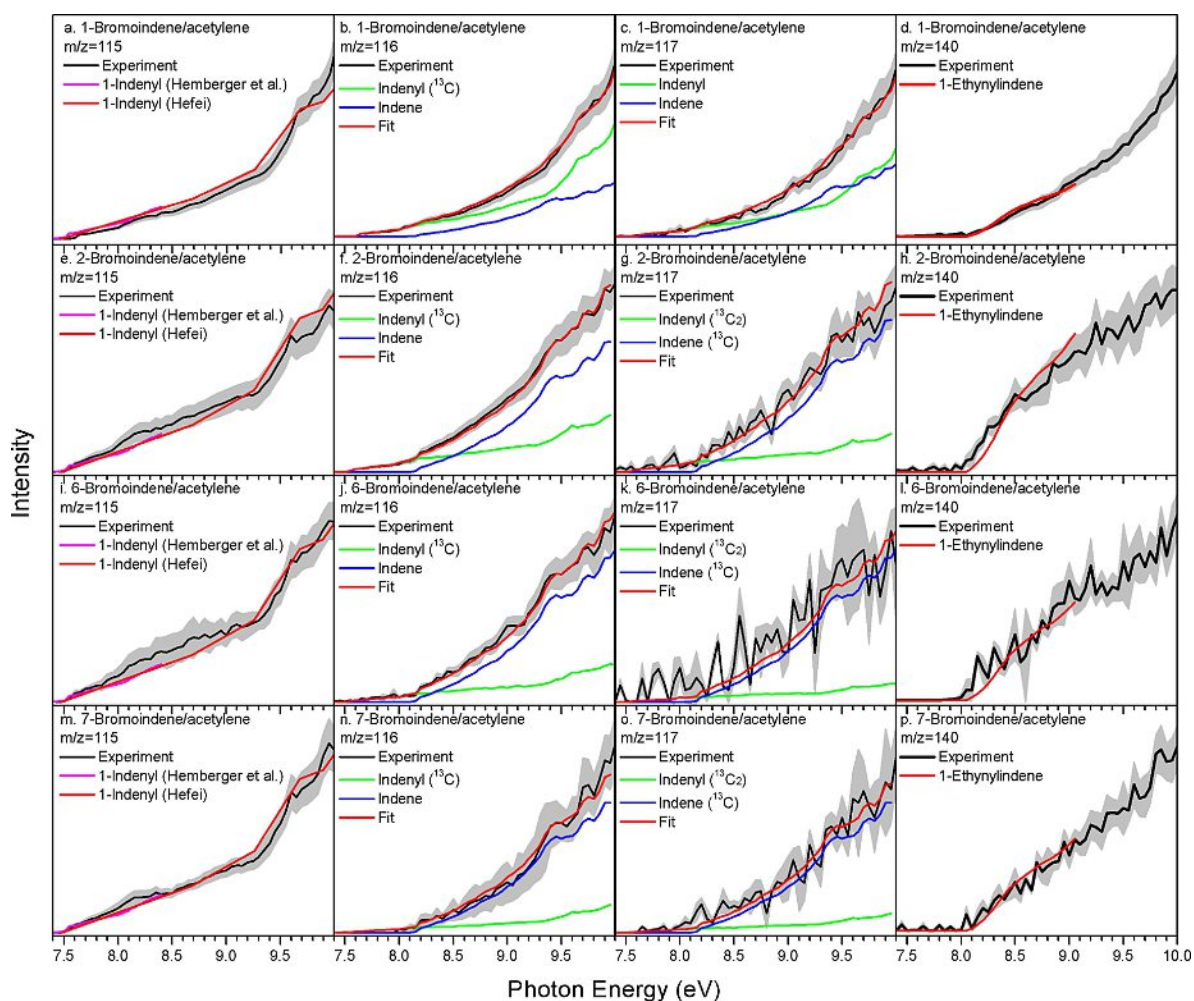


Figure 5. Experimental photoionization efficiency curves (PIE, black lines) for $m/z = 115, 116, 117$ and 140 in the reaction systems 1-bromoindene/acetylene (a–d), 2-bromoindene (e–h), 6-bromoindene (i–l), and 7-bromoindene (m–p), along with the experimental error (gray area) and the reference PIE curves (blue, green, purple and red lines). In the case of multiple contributions to one PIE curve, the red line resembles the overall fit. In the case for $m/z = 115$, both the purple and red lines represent reference PIE curves of 1-indenyl radical from Hemberger et al.'s work and Hefei database, respectively.

atures of up to 1,500 K as present in the reactor. Figure 6a compiles the results at a pressure of 76 Torr, which represents a typical pressure within the micro reactor.^[31] For other pressures, the switch between the third-body stabilization of indene and the production of 1-indenyl plus atomic hydrogen happens at different temperatures: the higher the pressure, the higher the temperature, where this switch occurs. The calculated life time of thermalized indene at 1,500 K and 76 Torr within the reactor is 279 μs but chemically activated indene initially formed from the association of 1-, 2-, 6-, and 7-indenyl radicals with hydrogen should be much shorter-lived. Indene practically exclusively dissociates to 1-indenyl plus atomic hydrogen, with the branching ratio of not below 99.9%. Overall, these reactions are exoergic by 144, 133, and 132 kJ mol^{-1} for the hydrogen assisted isomerization of 2-, 6-, and 7-indenyl radicals, respectively, to 1-indenyl. Therefore, our computations show that the 2-, 6-, and 7-indenyl radicals would isomerize to 1-indenyl via hydrogen addition – hydrogen elimination with rate constants close to $10^{-10} \text{ cm}^3 \text{ molecule}^{-1} \text{ s}^{-1}$ under our experimental con-

ditions. The calculated results of an atomic hydrogen loss from chemically activated indene molecules correlate with previous shock tube studies proposing 1-indenyl radical formation as the initial decomposition step^[32] and with a photochemical activation of indene at 193 nm indicating that indene decomposes via atomic hydrogen loss from the CH_2 moiety yielding the 1-indenyl radical exclusively; Bersohn et al. determined the lifetime of photochemically activated indene to be about 0.13 μs .^[33]

An alternative pathway leading from 2-, 6-, and 7-indenyl radicals to 1-indenyl would involve a series of hydrogen atom migrations. A typical H shift process in a polyaromatic radical is the one leading from 1-naphthyl to 2-naphthyl which features a high barrier of 251 kJ mol^{-1} and the life time for this isomerization to occur under the reactor conditions is $\sim 20 \mu\text{s}$.^[34] Depending on the concentration of hydrogen atoms present, the sequential hydrogen shift isomerization process would compete with the hydrogen assisted isomerization via indene. Considering the rate constant for the hydrogen assisted isomer-

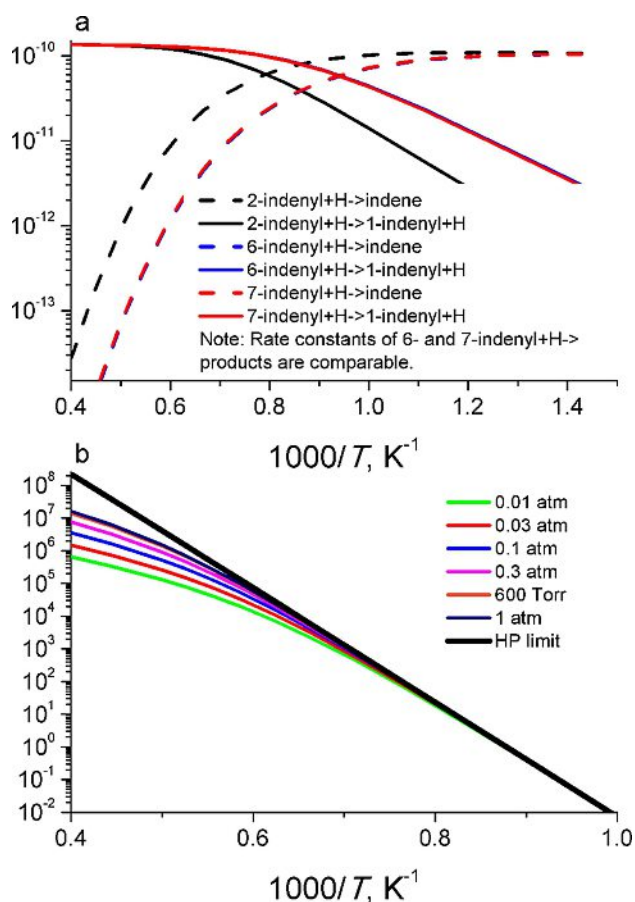


Figure 6. Calculated rate constants for the reactions of 2-, 6-, and 7-indenyl radicals with atomic hydrogen (top) and unimolecular indene decomposition (bottom).

ization to be $\sim 10^{-10} \text{ cm}^3 \text{ molecule}^{-1} \text{ s}^{-1}$ at 1500 K and above (Figure 6), the hydrogen assisted mechanism would prevail over the hydrogen migration pathway at hydrogen atom densities exceeding $5 \times 10^{14} \text{ cm}^{-3}$.

We need to also consider the rates of the *n*-indenyl plus hydrogen and *n*-indenyl + acetylene reactions because, if the latter is faster, some *n*-ethynylindenes ($n > 1$) should form if *n*-indenyls were initially generated. Let us consider the reactions of the indenyl radicals with acetylene leading to *n*-ethynylindenes plus atomic hydrogen. The inherent barriers of acetylene addition to 2- to 7-indene are rather low, 11 to 14 kJ mol⁻¹, and the resulting rate constants of 4.87×10^{-12} to 1.66×10^{-11} suggest that the hydrogen atom assisted isomerization of the 2- to 7-indenyl radical to 1-indenyl is faster by factors of 6 to 20 compared to the reaction of 2- to 7-indenyl with acetylene via addition followed by hydrogen loss to the corresponding *n*-ethynylindene products. Therefore, if the concentration of hydrogen atoms is comparable to that of acetylene, indenyl radicals generated in the pyrolysis of bromoindene predominantly isomerize to 1-indenyl in strongly exoergic reactions as discussed above rather than reacting with acetylene to 2- to 7-ethynylindenes. However, the fact that concentrations of hydrogen and acetylene are close is highly unlikely because the only

plausible source of hydrogen atoms is the initial bromoindene molecule and its concentration in the molecular beam is 3 orders of magnitude lower (0.1%) than that of neat acetylene. In this view, the initial formation of *n*-indenyl radicals from *n*-bromoindenes likely has to be ruled out because no *n*-ethynylindene products with $n > 1$ were observed.

Why do *n*-indenyl radicals ($n > 1$) not form from *n*-bromoindenes? The answer to this question lies in the comparison of the C–H and C–Br bond strengths in these molecules. The calculated C–H bond strengths in the CH₂ group of 2- and 7-bromoindenes are 332 and 329 kJ mol⁻¹, similar to the corresponding bond strength in unsubstituted indene, 327 kJ mol⁻¹. The C–Br bond energies in these bromoindenes are significantly higher, 368 and 360 kJ mol⁻¹. Note that the experimental C–Br bond strength in bromobenzene based on Active Thermochemical Tables is somewhat lower, 342 kJ mol⁻¹.^[35] However, even if the C–Br bond energy is slightly overestimated in our calculations, this bond remains stronger than C–H bonds in the CH₂ group. Therefore, dissociation of *n*-bromoindenes to the C₉H₆Br radicals plus an H atom should prevail over the C₉H₇[•] + Br channel for $n > 1$. Then, 1-indenyl should be formed as a major product via H-by-Br substitution as illustrated on the potential energy diagram shown in Figure 7. The hydrogen atom can approach the Br-linked carbon in *n*-bromoinden-1-yl radicals without a barrier and then the bromine atom is eliminated without an exit barrier to produce 1-indenyl plus bromine in the reactions which are exoergic overall by 101–107 kJ mol⁻¹. Similar to the hydrogen assisted isomerization of *n*-indenyl radicals to 1-indenyl, the H-by-Br substitution reactions converting *n*-bromoinden-1-yl radicals to 1-indenyl are expected to be fast, with rate constants in the range of $10^{-10} \text{ cm}^3 \text{ molecule}^{-1}$. Based on this consideration,

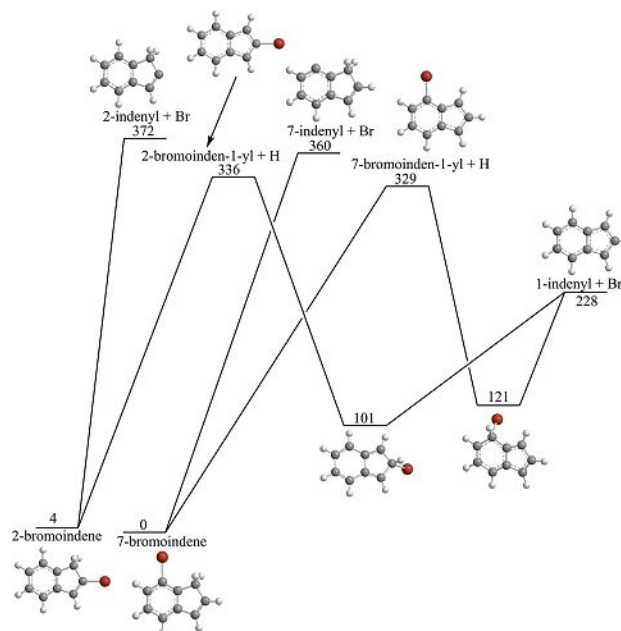


Figure 7. Calculated potential energy diagram for the decomposition of 2- and 7-bromoindenes and the formation of the 1-indenyl radical. All relative energies are shown in kJ mol⁻¹.

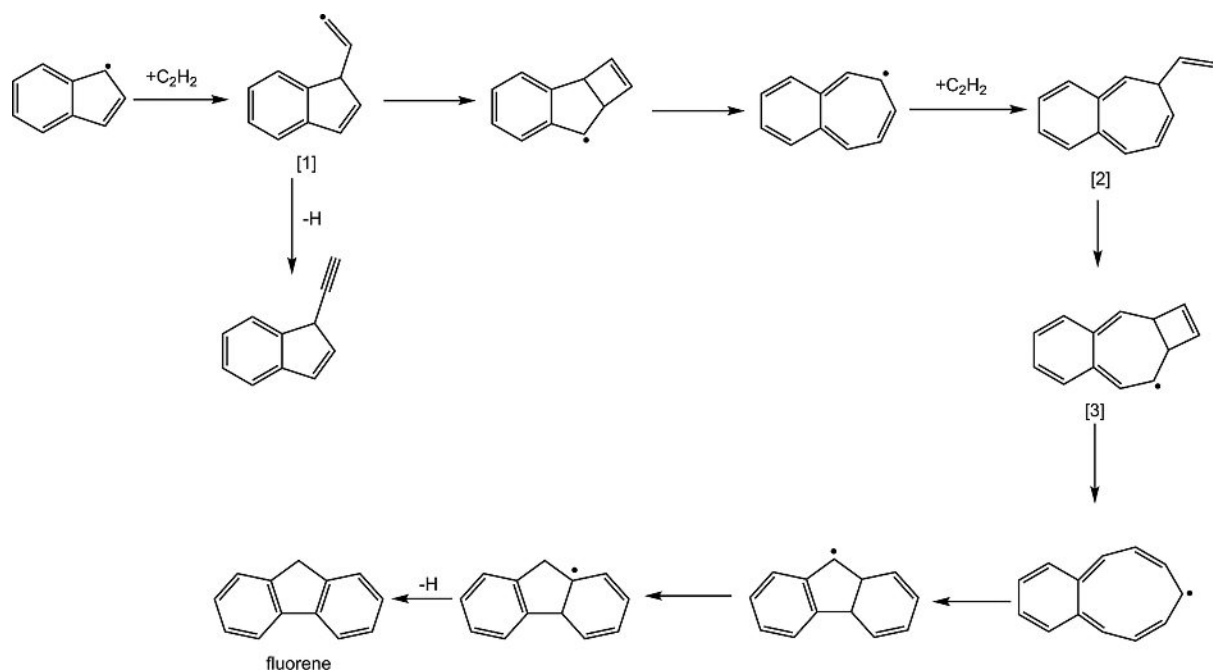


Figure 8. Reaction sequences of 1-indenyl with acetylene addition followed by H atom-loss forming 1-ethynylindene, and 1-indenyl with two-step acetylene addition generating fluorene followed by hydrogen loss.

we conclude that the most likely scenario for the formation of 1-indenyl from *n*-bromoindene is a two-step process in which the C–H bond cleavage producing *n*-bromoinden-1-yl is followed by the H-by-Br substitution. Thus, it can be concluded that *n*-bromoindenes ($n > 1$) do not represent appropriate precursors of *n*-indenyl radicals but rather work as indirect precursors of 1-indenyl.

Once the thermodynamically most stable 1-indenyl isomer is formed in all systems, 1-indenyl can react via Equation (R1) in an overall endoergic reaction ($+114 \text{ kJ mol}^{-1}$) synthesizing 1-ethynylindene. It is important to recall that no higher molecular weight reaction product than 1-ethynylindene (C_{11}H_8 ; 140 amu) could be probed in the acetylene systems. Therefore, rather than isomerization of the initial collision complex $\mathbf{i1}'$ to a more stable structure $\mathbf{i3}'$ containing two fused six- and seven-member rings followed by adding a second acetylene molecule to via a barrier of about 88 kJ mol^{-1} yielding intermediate [2] (Figure 8),^[17] intermediate $\mathbf{i1}'$ /[1] decomposes to 1-ethynylindene plus atomic hydrogen, and the route synthesizing fluorene via acetylene addition to $\mathbf{i3}'$ followed by ring closure to intermediate [3] and an eventual aromatization to fluorene ($\text{C}_{13}\text{H}_{10}$) via atomic hydrogen loss is closed (Figure 8). This experimental finding seems to contradict the calculated PES for the 1-indenyl plus acetylene reaction (Figure 2), which shows that the pathway to $\mathbf{i3}'$ is more energetically favorable than to 1-ethynylindene. The explanation why $\mathbf{i3}'$ does not react further with acetylene forming fluorene comes from the analysis of the rate constants and equilibrium constants in the 1-indenyl plus acetylene system. At 1500 K and in the 0.01 to 0.1 atm pressure range typical inside the reactor, the calculated rate constant to form 1-ethynylindene plus hydrogen is about $3.7 \times$

$10^{-17} \text{ cm}^3 \text{ molecule}^{-1} \text{ s}^{-1}$, whereas that to produce the collisionally stabilized (thermalized) intermediate $\mathbf{i3}'$ is higher by factors of 3.8 to 12.8, with the difference increasing with pressure. Thus, the formation of $\mathbf{i3}'$ is indeed more favorable. On the other hand, under the reactor conditions, the rate constant for the decomposition of $\mathbf{i3}'$ back to the 1-indenyl plus acetylene reactants are high, 8.6×10^4 – $2.7 \times 10^5 \text{ s}^{-1}$ corresponding to the life times of $\mathbf{i3}'$ of 3–12 μs , which are significantly shorter than the residence time in the reactor. It is therefore likely that the equilibrium is established between 1-indenyl plus acetylene and $\mathbf{i3}'$, with the computed equilibrium constant $K = [\mathbf{i3}']/([1\text{-indenyl}][\text{C}_2\text{H}_2])$ being $1.82 \times 10^{-21} \text{ cm}^3 \text{ molecule}^{-1}$. Using the upper estimate for $[\text{C}_2\text{H}_2]$ as $9.7 \times 10^{18} \text{ molecule cm}^{-3}$ corresponding to the pressure of 300 Torr and room temperature in the entrance of the reactor, we evaluate the $[\mathbf{i3}']/[1\text{-indenyl}]$ ratio to be below 0.018. The fact that only a tiny amount of $\mathbf{i3}'$ can survive and that the barrier for the $\mathbf{i3}'$ plus acetylene reaction is high, can account for the non-observation of fluorene.

Likewise, the reaction of the 1-indenyl radical with vinylacetylene did not lead to any fluorene ($\text{C}_{13}\text{H}_{10}$) formation via vinylacetylene addition to the radical center in 1-indenyl followed by isomerization via hydrogen shifts/ring closure and aromatization via hydrogen atom loss to fluorene ($\text{C}_{13}\text{H}_{10}$) because of the high critical barrier for this pathway (132 kJ mol^{-1}), which is even higher than the barriers to form the 1-((*E*)-but-1-en-3-ynyl)-1*H*-indene (**p1**) and 1-(but-3-en-1-ynyl)-1*H*-indene (**p2**) products, 128 and 123 kJ mol^{-1} , respectively. According to RRKM-ME calculations, **p1** and **p2** are practically exclusive reaction products with rate constants of 4.5×10^{-18} and $4.4 \times 10^{-17} \text{ cm}^3 \text{ molecule}^{-1} \text{ s}^{-1}$ at 1500 K, respec-

tively, whereas the production of fluorene and its 1*H*-cyclopenta[*a*]naphthalene isomer is negligible. With rate constants to form the C₁₃H₁₀ products being so low and the concentration of C₄H₄ in the He/C₄H₄ beam being a factor of 20 lower as compared to the concentration of acetylene in the neat acetylene beam, it becomes clear why no products of the 1-indenyl plus vinylacetylene reaction were observed at all.

4. Conclusions

In conclusion, our combined experimental and computational study revealed the exclusive formation of the resonantly stabilized 1-indenyl radical (C₉H₇[•]) upon the pyrolytic decomposition of 1-, 2-, 6-, and 7-bromoindenes. Once the thermodynamically most stable 1-indenyl radical was produced, reaction with acetylene yielded 1-ethynylindene plus atomic hydrogen via an initial addition of the 1-indenyl radical with its radical center to the acetylenic carbon atom yielding the *i1'* doublet intermediate via an entrance barrier of 60 kJ mol⁻¹. Rather than adding a second acetylene molecule and accessing potential routes to fluorene (C₁₃H₁₀), *i1'* underwent unimolecular decomposition to 1-ethynylindene. While this reaction mechanism is analogous to the bimolecular reaction between the phenyl radical (C₆H₅[•]) and acetylene (C₂H₂) forming phenylacetylene (C₆H₅CCH),^[22,36] the 1-indenyl plus acetylene → 1-ethynylindene plus hydrogen reaction is highly endoergic (114 kJ mol⁻¹) and slow, on the contrary to the exoergic (-38 kJ mol⁻¹) and much faster (by nearly 5 orders of magnitude at 1500 K) C₆H₅ + C₂H₂ → C₆H₅CCH + H reaction.^[34] Therefore, the 1-indenyl radical appears not to be an efficient precursor for further PAH growth either via HACA or HAVA mechanisms, but could be part of yet unknown reaction pathways to molecular growth, possibly involving the radical-radical reaction between 1-indenyl and methyl leading eventually to naphthalene (Reaction (R2)).^[2e]



Experimental and Computational Section

The experiments were conducted at the Chemical Dynamics Beamline (9.0.2) of the Advanced Light Source exploiting a resistively-heated silicon-carbide (SiC) chemical reactor interfaced to a molecular beam apparatus operated with a reflectron time-of-flight mass spectrometer (Re-TOF-MS).^[2f,14a,22–23,25a,c,27,30,37] First, we determine the nature of the indenyl radical isomer(s) formed (and potential isomerization processes); thereafter we study the reaction of the characterized indenyl radical(s) with acetylene (C₂H₂) and vinylacetylene (C₄H₄). The chemical reactor replicates the high temperature conditions along with discrete chemical reactions in situ through the generation and reaction of distinct radicals. Here, indenyl radicals (C₉H₇[•]) were generated at concentrations of less than 0.1% in situ via pyrolysis of 1-bromoindene, 2-bromoindene, 6-bromoindene, and 7-bromoindene precursors (C₉H₇Br; 99%; Sigma Aldrich, excluding 1-bromoindene) seeded in acetylene carrier gas (99.6%; Matheson Gas). The 1-bromoindene precursor was synthesized using a modified procedure from the literature,^[38] details and characterization are provided in the Supplementary Information. The temperature of the silicon carbide tube was monitored using a Type-C thermocouple and held at 1500 ± 10 K;

inlet pressures of the acetylene carrier gas were regulated to be 300 Torr. The products formed in the reactor were expanded supersonically and passed through a 2 mm diameter skimmer located 10 mm downstream of the pyrolytic reactor and enter into the main chamber, which hosts the ReTOF-MS. The quasi-continuous tunable VUV light from the Advanced Light Source intersects the neutral molecular beam perpendicularly in the extraction region of a Wiley-McLaren Re-TOF-MS. VUV single photon ionization represents basically a fragment-free ionization technique and hence is considered as a *soft ionization* method compared to electron impact ionization.^[2f,14a,22–23,25a,c,27,30,37,39] The ions generated in the photoionization process are extracted and fed onto a microchannel plate detector through an ion lens. PIE curves, which report ion counts as a function of photon energy from 7.40 eV to 10.00 eV with a step interval of 0.05 eV at a well-defined mass-to-charge ratio (*m/z*), were produced by integrating the signal recorded at the specific *m/z* for the species of interest. The PI curves presented herein are the average of multiple acquisitions with the shaded area representing 1σ uncertainty including the 10% error signal measurement from the calibrated photodiode, which monitored the intensity of the VUV beam. Hereafter, the neat acetylene (C₂H₂) was replaced by helium-seeded vinylacetylene (C₄H₄) at identical temperature (1500 ± 10 K) and pressures (300 Torr) to probe the reaction products of the indenyl radical(s) with vinylacetylene. The helium-vinylacetylene premix (5%) was acquired from Applied Gas Inc.

The calculations of the energies and molecular parameters of various indenyl radicals, their reaction energies with acetylene forming ethynylindene isomers along with atomic hydrogen, intermediates and transition states for the reactions of 1-indenyl with acetylene and vinylacetylene, and transition states for acetylene additions to the other indenyl isomers (from 2- to 7-indenyl) were carried out at the G3(MP2,CC)//B3LYP/6-311G(d,p) level of theory, where geometries are optimized and vibrational frequencies are calculated using the density functional B3LYP method with the 6-311G(d,p) method and single-point total energies are refined through a series of coupled clusters CCSD(T) and second-order Møller–Plesset perturbation theory MP2 calculations as $E[\text{G3}(\text{MP2,CC})] = E[\text{CCSD}(\text{T})/6-311\text{G}(\text{d,p})] + E[\text{MP2}/\text{G3Large}] - E[\text{MP2}/6-311\text{G}(\text{d,p})] + \text{ZPE}[\text{B3LYP}/6-311\text{G}(\text{d,p})]$.^[40] This model chemistry theoretical approach is chemically accurate since it provides accuracy of 0.01–0.02 Å for bond lengths, 1–2° for bond angles, and 3–6 kJ mol⁻¹ for relative energies of hydrocarbons, their radicals, and reaction energies in terms of average absolute deviations.^[40b] The GAUSSIAN 09^[41] and MOLPRO 2010^[42] program packages were utilized for the ab initio calculations. Vertical and adiabatic ionization energies of the indenyl radicals and of the ethynyl-indene isomers were also computed at the G3(MP2,CC)//B3LYP/6-311G(d,p) level of theory.

Rate constants of the indenyl + H/C₂H₂/C₄H₄ reactions and related reactions on the C₉H₈, C₁₁H₉, and C₁₃H₁₁ potential energy surfaces (PES) at various temperatures and pressures were computed using the Rice-Ramsperger-Kassel-Marcus Master Equation (RRKM-ME) theoretical approach as implemented in the MESS software package.^[43] The Rigid-Rotor, Harmonic-Oscillator (RRHO) model was generally adopted for the calculations of densities of states and partition functions for local minima and numbers of states for transition states. Additional details of RRKM-ME calculations can be found in our previous publications.^[5,7] For the barrier-less C₉H₇ + H entrance channels, we used phase space theory^[44] to fit their high-pressure limit rate constants to the most accurate values either for C₅H₅ + H → C₅H₆ (for 1-indenyl) or for C₆H₅ + H → C₆H₆ (for *n*-indenyl with *n* > 1) calculated by Klippenstein and co-workers^[45] using variable reaction coordinate transition state theory (VRC-TST). Then,

these high-pressure limit rate constants were utilized in RRKM-ME calculations to determine the pressure dependence.

Acknowledgements

This work was supported by the US Department of Energy, Basic Energy Sciences DE-FG02-03ER15411 (University of Hawaii), DE-FG02-04ER15570 (Florida International University). B.X., U.A., W.L and M.A. are supported by the Director, Office of Science, Office of Basic Energy Sciences, of the U.S. Department of Energy under Contract No. DE-AC02-05CH11231, through the Gas Phase Chemical Physics program in the Chemical Sciences Division. The ALS is supported under the same contract. Ab initio and RRKM-ME calculations at Samara University were supported by the Ministry of Higher Education and Science of the Russian Federation under Grant No. 14.Y26.31.0020.

Conflict of Interest

The authors declare no conflict of interest.

Keywords: ab initio calculations · gas-phase chemistry · hydrogen abstraction–acetylene addition (HACA) · mass spectrometry · polycyclic aromatic hydrocarbons

- [1] K. Johansson, M. Head-Gordon, P. Schrader, K. Wilson, H. Michelsen, *Science* **2018**, *361*, 997–1000.
- [2] a) V. V. Kislov, A. M. Mebel, J. Aguilera-Iparraguirre, W. H. Green, *J. Phys. Chem. A* **2012**, *116*, 4176–4191; b) H. Nakamura, R. Tanimoto, T. Tezuka, S. Hasegawa, K. Maruta, *Combust. Flame* **2014**, *161*, 582–591; c) P. Constantinidis, H. C. Schmitt, I. Fischer, B. Yan, A. M. Rijs, *Phys. Chem. Chem. Phys.* **2015**, *17*, 29064–29071; d) C. Wentrup, H. W. Winter, D. Kvaskoff, *J. Phys. Chem. A* **2015**, *119*, 6370–6376; e) A. M. Mebel, Y. Georgievskii, A. W. Jasper, S. J. Klippenstein, *Faraday Discuss.* **2016**, *195*, 637–670; f) D. S. N. Parker, R. I. Kaiser, O. Kostko, M. Ahmed, *ChemPhysChem* **2015**, *16*, 2091–2093; g) A. M. Mebel, A. Landera, R. I. Kaiser, *J. Phys. Chem. A* **2017**, *121*, 901–926; h) D. S. Parker, F. Zhang, R. I. Kaiser, V. V. Kislov, A. M. Mebel, *Chem. Asian J.* **2011**, *6*, 3035–3047; i) B. Shukla, M. Koshi, *Combust. Flame* **2011**, *158*, 369–375.
- [3] a) A. L. Lafleur, J. B. Howard, J. A. Marr, T. Yadav, *J. Phys. Chem.* **1993**, *97*, 13539–13543; b) N. S. Goroff, *Acc. Chem. Res.* **1996**, *29*, 77–83; c) A. L. Lafleur, J. B. Howard, K. Taghizadeh, E. F. Plummer, L. T. Scott, A. Neucula, K. C. Swallow, *J. Phys. Chem.* **1996**, *100*, 17421–17428.
- [4] T. R. Melton, A. M. Vincitore, S. M. Senkan, *Proc. Combust. Inst.* **1998**, *27th*, 1631–1637.
- [5] T. R. Melton, F. Inal, S. M. Senkan, *Combust. Flame* **2000**, *121*, 671–678.
- [6] Y. Li, L. Zhang, Z. Tian, T. Yuan, K. Zhang, B. Yang, F. Qi, *Proc. Combust. Inst.* **2009**, *32*, 1293–1300.
- [7] M. Kamphus, M. Braun-Unkhoff, K. Kohse-Höinghaus, *Combust. Flame* **2008**, *152*, 28–59.
- [8] N. Marinov, W. Pitz, C. Westbrook, A. Lutz, A. Vincitore, S. Senkan, *Proc. Combust. Inst.* **1998**, *27*, 605–613.
- [9] J. J. Newby, J. A. Stearns, C.-P. Liu, T. S. Zwier, *J. Phys. Chem. A* **2007**, *111*, 10914–10927.
- [10] Y. Li, L. Zhang, T. Yuan, K. Zhang, J. Yang, B. Yang, F. Qi, C. K. Law, *Combust. Flame* **2010**, *157*, 143–154.
- [11] a) Y. Li, L. Zhang, Z. Tian, T. Yuan, J. Wang, B. Yang, F. Qi, *Energy Fuels* **2009**, *23*, 1473–1485; b) T. Zhang, L. Zhang, X. Hong, K. Zhang, F. Qi, C. K. Law, T. Ye, P. Zhao, Y. Chen, *Combust. Flame* **2009**, *156*, 2071–2083.
- [12] a) D. H. Kim, J. A. Mulholland, D. Wang, A. Violi, *J. Phys. Chem. A* **2010**, *114*, 12411–12416; b) A. Lamprecht, B. Atakan, K. Kohse-Höinghaus, *Proc. Combust. Inst.* **2000**, *28*, 1817–1824.
- [13] D. Wang, A. Violi, D. H. Kim, J. A. Mulholland, *J. Phys. Chem. A* **2006**, *110*, 4719–4725.
- [14] a) F. Zhang, R. I. Kaiser, V. V. Kislov, A. M. Mebel, A. Golan, M. Ahmed, *J. Phys. Chem. Lett.* **2011**, *2*, 1731–1735; b) A. M. Turner, M. J. Abplanalp, S. Y. Chen, Y. T. Chen, A. H. H. Chang, R. I. Kaiser, *Phys. Chem. Chem. Phys.* **2015**, *17*, 27281–27291.
- [15] P. Lindstedt, L. Maurice, M. Meyer, *Faraday Discuss.* **2001**, *119*, 409–432.
- [16] K. Mati, A. Ristori, G. Pengloan, P. Dagaut, *Combust. Sci. Technol.* **2007**, *179*, 1261–1285.
- [17] C. Cavallotti, S. Mancarella, R. Rota, S. Carra, *J. Phys. Chem. A* **2007**, *111*, 3959–3969.
- [18] R. F. Pottier, F. P. Lossing, *J. Am. Chem. Soc.* **1963**, *85*, 269–271.
- [19] P. Hemberger, M. Steinbauer, M. Schneider, I. Fischer, M. Johnson, A. Bodi, T. Gerber, *J. Phys. Chem. A* **2010**, *114*, 4698–4703.
- [20] *Photonization Cross Section Database (Version 2.0)*, National Synchrotron Radiation Laboratory, Hefei, China, <http://flame.nsl.ustc.edu.cn/database/> (2017).
- [21] B. West, A. Sit, A. Bodi, P. Hemberger, P. M. Mayer, *J. Phys. Chem. A* **2014**, *118*, 11226–11234.
- [22] D. S. Parker, R. I. Kaiser, T. P. Troy, M. Ahmed, *Angew. Chem. Int. Ed.* **2014**, *53*, 7740–7744; *Angew. Chem.* **2014**, *126*, 7874–7878.
- [23] a) T. Yang, L. Muzangwa, R. I. Kaiser, A. Jamal, K. Morokuma, *Phys. Chem. Chem. Phys.* **2015**, *17*, 21564–21575; b) D. S. Parker, F. Zhang, Y. S. Kim, R. I. Kaiser, A. Landera, V. V. Kislov, A. M. Mebel, A. Tielens, *Proc. Natl. Acad. Sci. USA* **2012**, *109*, 53–58; c) D. S. N. Parker, B. B. Dangi, R. I. Kaiser, A. Jamal, M. N. Ryazantsev, K. Morokuma, A. Korte, W. Sander, *J. Phys. Chem. A* **2014**, *118*, 2709–2718; d) L. Zhao, R. I. Kaiser, B. Xu, U. Ablikim, M. Ahmed, M. V. Zagidullin, V. N. Azyazov, A. H. Howlader, S. F. Wnuk, A. M. Mebel, *J. Phys. Chem. Lett.* **2018**, *9*, 2620–2626.
- [24] a) L. Zhao, T. Yang, R. I. Kaiser, T. P. Troy, M. Ahmed, D. Belisario-Lara, J. M. Ribeiro, A. M. Mebel, *J. Phys. Chem. A* **2017**, *121*, 1261–1280; b) L. Zhao, T. Yang, R. I. Kaiser, T. P. Troy, M. Ahmed, J. M. Ribeiro, D. Belisario-Lara, A. M. Mebel, *J. Phys. Chem. A* **2017**, *121*, 1281–1297.
- [25] a) O. Kostko, J. Zhou, B. J. Sun, J. S. Lie, A. H. H. Chang, R. I. Kaiser, M. Ahmed, *Astrophys. J.* **2010**, *717*, 674–682; b) P. Maksyutenko, M. Förstel, P. Crandall, B.-J. Sun, M.-H. Wu, A. H. H. Chang, R. I. Kaiser, *Chem. Phys. Lett.* **2016**, *658*, 20–29; c) R. I. Kaiser, B. J. Sun, H. M. Lin, A. H. H. Chang, A. M. Mebel, O. Kostko, M. Ahmed, *Astrophys. J.* **2010**, *719*, 1884–1889.
- [26] R. Schulz, A. Schweig, C. Wentrup, H. W. Winter, *Angew. Chem. Int. Ed.* **1980**, *19*, 821–822; *Angew. Chem.* **1980**, *92*, 846–847.
- [27] D. S. N. Parker, R. I. Kaiser, B. Bandyopadhyay, O. Kostko, T. P. Troy, M. Ahmed, *Angew. Chem. Int. Ed.* **2015**, *54*, 5421–5424; *Angew. Chem.* **2015**, *127*, 5511–5514.
- [28] L. Zhao, R. I. Kaiser, B. Xu, U. Ablikim, M. Ahmed, D. Joshi, G. Veber, F. R. Fischer, A. M. Mebel, *Nat. Astron.* **2018**, *2*, 413–419.
- [29] M. V. Zagidullin, R. I. Kaiser, D. Porfiriev, I. P. Zavershinskiy, M. Ahmed, V. N. Azyazov, A. M. Mebel, *J. Phys. Chem. A* **2018**, *122*, 8819–8827.
- [30] F. T. Zhang, R. I. Kaiser, A. Golan, M. Ahmed, N. Hansen, *J. Phys. Chem. A* **2012**, *116*, 3541–3546.
- [31] K. N. Urness, Q. Guan, A. Golan, J. W. Daily, M. R. Nimlos, J. F. Stanton, M. Ahmed, G. B. Ellison, *J. Chem. Phys.* **2013**, *139*, 124305.
- [32] a) A. Laskin, A. Lifshitz, *Proc. Combust. Inst.* **1998**, *27th*, 313–320; b) A. Burcat, M. Dvinyaninov, *Int. J. Chem. Kinet.* **1997**, *29*, 505–514; c) K. Roy, P. Frank, T. Just, *Isr. J. Chem.* **1996**, *36*, 275–278.
- [33] W. Yi, A. Chattopadhyay, R. Bersohn, *J. Chem. Phys.* **1991**, *94*, 5994–5998.
- [34] A. M. Mebel, Y. Georgievskii, A. W. Jasper, S. J. Klippenstein, *Proc. Combust. Inst.* **2017**, *36*, 919–926.
- [35] B. Ruscic, *Vol. Active Thermochemical Tables, Version 1.122*, available at <http://atct.anl.gov>.
- [36] X. Gu, F. Zhang, Y. Guo, R. I. Kaiser, *Angew. Chem. Int. Ed.* **2007**, *46*, 6866–6869; *Angew. Chem.* **2007**, *119*, 6990–6993.
- [37] a) R. I. Kaiser, L. Belau, S. R. Leone, M. Ahmed, Y. M. Wang, B. J. Braams, J. M. Bowman, *ChemPhysChem* **2007**, *8*, 1236–1239; b) R. I. Kaiser, A. Mebel, O. Kostko, M. Ahmed, *Chem. Phys. Lett.* **2010**, *485*, 281–285; c) R. I. Kaiser, S. P. Krishtal, A. M. Mebel, O. Kostko, M. Ahmed, *Astrophys. J.* **2012**, *761*, 178–184; d) A. Golan, M. Ahmed, A. M. Mebel, R. I. Kaiser, *Phys. Chem. Chem. Phys.* **2013**, *15*, 341–347.
- [38] J. A. Murphy, C. W. Patterson, *J. Chem. Soc. Perkin Trans. 1* **1993**, 405–410.
- [39] a) F. Qi, R. Yang, B. Yang, C. Q. Huang, L. X. Wei, J. Wang, L. S. Sheng, Y. W. Zhang, *Rev. Sci. Instrum.* **2006**, *77*, 084101; b) B. Yang, Y. Y. Li, L. X. Wei, C. Q. Huang, J. Wang, Z. Y. Tian, R. Yang, L. S. Sheng, Y. W. Zhang, F. Qi, *Proc. Combust. Inst.* **2007**, *31*, 555–563; c) B. Yang, P. Oßwald, Y. Li, J. Wang, L. Wei, Z. Tian, F. Qi, K. Kohse-Höinghaus, *Combust. Flame* **2007**, *148*, 198–209; d) Y. Y. Li, L. D. Zhang, Z. Y. Tian, T. Yuan, J. Wang,

- B. Yang, F. Qi, *Energy Fuels* **2009**, *23*, 1473–1485; e) Y. Y. Li, L. D. Zhang, Z. Y. Tian, T. Yuan, K. W. Zhang, B. Yang, F. Qi, *Proc. Combust. Inst.* **2009**, *32*, 1293–1300; f) L. D. Zhang, J. H. Cai, T. C. Zhang, F. Qi, *Combust. Flame* **2010**, *157*, 1686–1697; g) P. Oßwald, H. Güldenbergh, K. Kohse-Höinghaus, B. Yang, T. Yuan, F. Qi, *Combust. Flame* **2011**, *158*, 2–15; h) F. Qi, *Proc. Combust. Inst.* **2013**, *34*, 33–63.
- [40] a) L. A. Curtiss, K. Raghavachari, P. C. Redfern, V. Rassolov, J. A. Pople, *J. Chem. Phys.* **1998**, *109*, 7764–7776; b) L. A. Curtiss, K. Raghavachari, P. C. Redfern, A. G. Baboul, J. A. Pople, *Chem. Phys. Lett.* **1999**, *314*, 101–107; c) A. G. Baboul, L. A. Curtiss, P. C. Redfern, K. Raghavachari, *J. Chem. Phys.* **1999**, *110*, 7650–7657.
- [41] M. J. Frisch, G. W. Trucks, H. B. Schlegel, G. E. Scuseria, M. A. Robb, J. R. Cheeseman, G. Scalmani, V. Barone, B. Mennucci, G. A. Petersson, H. Nakatsuji, M. Caricato, X. Li, H. P. Hratchian, A. F. Izmaylov, J. Bloino, G. Zheng, J. L. Sonnenberg, M. Hada, M. Ehara, K. Toyota, R. Fukuda, J. Hasegawa, M. Ishida, T. Nakajima, Y. Honda, O. Kitao, H. Nakai, T. Vreven, J. A. Montgomery, Jr., J. E. Peralta, F. Ogliaro, M. Bearpark, J. J. Heyd, E. Brothers, K. N. Kudin, V. N. Staroverov, T. Keith, R. Kobayashi, J. Normand, K. Raghavachari, A. Rendell, J. C. Burant, S. S. Iyengar, J. Tomasi, M. Cossi, N. Rega, J. M. Millam, M. Klene, J. E. Knox, J. B. Cross, V. Bakken, C. Adamo, J. Jaramillo, R. Gomperts, R. E. Stratmann, O. Yazyev, A. J. Austin, R. Cammi, C. Pomelli, J. W. Ochterski, R. L. Martin, K. Morokuma, V. G. Zakrzewski, G. A. Voth, P. Salvador, J. J. Dannenberg, S. Dapprich, A. D. Daniels, O. Farkas, J. B. Foresman, J. V. Ortiz, J. Cioslowski, D. J. Fox, *Revision A.1 Gaussian Inc., Wallingford CT* **2009**.
- [42] H. J. Werner, P. J. Knowles, G. Knizia, F. R. Manby, M. Schütz, P. Celani, W. Györfly, D. Kats, T. Korona, R. Lindh, A. Mitrushenkov, G. Rauhut, K. R. Shamasundar, T. B. Adler, R. D. Amos, A. Bernhardsson, A. Berning, D. L. Cooper, M. J. O. Deegan, A. J. Dobbyn, F. Eckert, E. Goll, C. Hampel, A. Hesselmann, G. Hetzer, T. Hrenar, G. Jansen, C. Köppl, Y. Liu, A. W. Lloyd, R. A. Mata, A. J. May, S. J. McNicholas, W. Meyer, M. E. Mura, A. Nicklaß, D. P. O'Neill, P. Palmieri, D. Peng, K. Pflüger, R. Pitzer, M. Reiher, T. Shiozaki, H. Stoll, A. J. Stone, R. Tarroni, T. Thorsteinsson, M. Wang, *MOLPRO, version 2010.1, a package of ab initio programs*, <http://www.molpro.net>.
- [43] a) Y. Georgievskii, J. A. Miller, M. P. Burke, S. J. Klippenstein, *J. Phys. Chem. A* **2013**, *117*, 12146–12154; b) Y. Georgievskii, S. J. Klippenstein, *Master Equation System Solver (MESS) available online at <http://tcg.cse.anl.gov/papr>* **2015**.
- [44] S. J. Klippenstein, J. I. Cline, *J. Chem. Phys.* **1995**, *103*, 5451–5460.
- [45] a) L. B. Harding, S. J. Klippenstein, Y. Georgievskii, *J. Phys. Chem. A* **2007**, *111*, 3789–3801; b) L. B. Harding, Y. Georgievskii, S. J. Klippenstein, *J. Phys. Chem. A* **2005**, *109*, 4646–4656.

Manuscript received: January 17, 2019
 Revised manuscript received: February 28, 2019
 Accepted manuscript online: April 2, 2019
 Version of record online: April 18, 2019